

# Quantum interferometry with complex molecules

MARKUS ARNDT

*Faculty of Physics, University of Vienna, Boltzmannngasse 5, 1090 Wien, Austria*

KLAUS HORNBERGER

*Department of Physics, LMU Munich, Theresienstraße 37, 80333 München, Germany*

**Summary.** — This chapter reviews recent experiments on matter wave interferometry with large molecules. Starting from an elementary introduction to matter wave physics we discuss far-field diffraction and near-field interferometry with thermally excited many-body systems. We describe the constraints imposed by decoherence and dephasing effects, and present an outlook to the future challenges in macro-molecule and cluster interferometry.

PACS 03.75.-b – Matter waves.

## 1. – Historical introduction and overview

The year 1923 is generally considered as the year of birth of matter wave physics. It is the year when Louis de Broglie proposed the idea that each material particle is accompanied by an oscillatory phenomenon [1]. De Broglie based his hypothesis on two discoveries: the *energy-frequency equivalence* for photons,  $E = \hbar\omega$ , and the *energy-mass equivalence* for matter,  $E = mc^2$ . While the first relation had already been central to Planck's explanation of the black body spectrum [2] and to Einstein's analysis of the photo effect [3], the latter was a consequence of Einstein's theory of special relativity.

The generalization of these two relations to material particles led Louis de Broglie to conclude that any object of mass  $m$  must be accompanied by an oscillatory phenomenon of frequency  $\omega = mc^2/\hbar$  [1]. If the material object moves at velocity  $v$  with regard to an observer at rest the Lorentz transformation, which mixes the position and time coordinates, implies that this oscillation appears as a propagating wave, whose wave length is determined by the de Broglie relation  $\lambda_{dB} = h/(mv)$ .

While this hypothesis could be immediately employed to explain the stability of the electron orbits in Bohr's model of the hydrogen atom, its formalization led to Schrödinger's wave equation [4], one of the cornerstones of modern physics. Empirical confirmations of the wave hypothesis were soon found in two experiments with free electron beams: In 1927 C. J. Davisson and L. Germer described interference in the *reflection* of an electron beam off a clean nickel crystal surface [5]. In the same year, G. P. Thomson [6] observed diffraction in the *transmission* of a free electron beam through a thin sheet of platinum.

Today, *electron interferometry* is an important element in the surface sciences [7]. Electron microscopes explicitly exploit the fact that fast electrons are associated with a de Broglie wavelength that can resolve surface structures down to the level of single atoms. The coherence properties of electrons can also be used to reveal the surface crystal structure in low-energy electron diffraction (*LEED*) [8]. Also holography, which was suggested for electrons first [9], is nowadays applied for advanced phase imaging in the materials sciences [10]. The electron wave nature is essential for the understanding of the working principle of the scanning tunneling microscope (*STM*) [11], as well as for the interpretation of advanced STM images [12]. Electron coherence is also the precondition for decoherence experiments in mesoscopic semiconductor structures [13] and with charges flying close to material surfaces [14, 15].

As indicated by the de Broglie relation  $\lambda_{dB} = h/(mv)$ , the observation of matter wave effects depends crucially on the speed and mass of the interfering particles. The smaller the mass and the velocity of the objects the easier it will be to observe wave phenomena. In addition, neutral particles are more accessible to interference compared to charged ones, since they are less susceptible to phase averaging and decoherence induced by residual electromagnetic fields.

The lightest *neutral particles* that were experimentally accessible at the beginning of the last century were the helium atom and the hydrogen molecule. I. Estermann and O. Stern were the first to demonstrate diffraction of He and H<sub>2</sub> at a crystal surface [16], which confirmed the de Broglie relation for composite objects. Two years after that the neutron was discovered by J. Chadwick [17], and already four years later the first successful neutron diffraction experiment was carried out [18].

Although it takes a nuclear reactor to generate an intense neutron beam, the methods of *coherent and incoherent neutron scattering*, pioneered by C. Shull [19] and B. Brockhouse [20], are nowadays routine tools in the field of condensed matter physics [21], as well as for experiments on the foundations of quantum optics [22]. They are particularly useful for the structural analysis of materials which are composed of light elements, such as carbon and hydrogen. These elements, which are ubiquitous in all organic materials,

are less accessible to x-ray imaging due to their limited number of electrons, but they are favorable candidates for neutron scattering since the masses of the lattice atoms and the scattered neutrons are not too different.

After the first demonstrations of atom diffraction it took nearly 60 years before *atom interferometry* was taken up again. The new experiments were spurred by the progress in the development of lasers and nano-fabrication methods as well as by advances in atom cooling techniques. In the mid-1980s, interference of atoms was demonstrated using standing laser light waves [23, 24], nano-fabricated gratings [25], and mechanical double slits [26]. Extensions to complete multi-grating atom interferometers became rapidly available [27, 28] and were applied to various new problems. This led to precision measurements of atomic polarizabilities [29, 30], of the Earth's gravitation [31, 32] and rotation [33, 34], of the atomic recoil during photon absorption [35], and the index of refraction for atoms passing through a dilute gas [36].

The extrapolation of matter wave interference to *diatomic molecules* was then realized in 1994 for  $I_2$  using optical recoil gratings in a Ramsey-Bordé configuration [37]. In the same year, far-field diffraction behind a nano-fabricated mask led to the discovery of the weakly bound He-dimer [38], and the MIT group extended their Mach-Zehnder interferometer experiments from sodium atoms to  $Na_2$  [39].

In 1995 the experimental realization of *Bose-Einstein condensates* then redirected a major part of atomic physics research towards the exciting field of ultra-cold quantum degenerate gases, also covered by two Varenna summer schools by now [40, 41]. A plethora of matter-wave phenomena was observed in these macroscopic quantum ensembles, and we refer the reader to the recent reviews and monographs in the field [42, 43, 44, 45, 46]. It is noteworthy that the interference phenomena observed with dilute Bose-Einstein condensates are single-atom effects, even though the condensate order parameter may represent the matter wave field of more than ten million atoms in a typical BEC experiment. In spite of this macroscopic number, the wave length associated with the solution of the Gross-Pitaevski equation is determined by the mass of the individual atoms alone. As a matter of fact, in all BEC experiments it is desired to isolate the atoms in a dilute gas in order to avoid larger aggregations during the cooling process.

The purpose of our present contribution is to introduce the reader to the coherent manipulation of *large molecules*, i.e., strongly bound ensembles of atoms which may be as hot as 2000 K. In these experiments, matter wave physics is extended into a mass and complexity domain where many molecular properties mimic features of bulk media rather than those of single atoms. This opens a way to detailed studies of the gradual transition from quantum phenomena to classical appearances, and it offers the possibility to measure properties of big molecules in advanced interferometric experiments.

## 2. – Elementary matter wave optics

Before we turn to the experiments of molecular quantum optics, it is worth emphasizing that many of the observations can be well understood by the concepts of classical wave optics. Our starting point is the Schrödinger equation since the energies and veloc-

ities involved remain safely on the non-relativistic side of physics. Let us first consider a stationary situation, as it is often encountered in interferometry, where the time dependence of both the beam source and the external potential can be ignored. In this case, one can establish a formal equivalence between the Schrödinger equation on the one hand, and the (generalized) Helmholtz equation for the propagation of light waves on the other hand.

Starting from the Schrödinger equation for a particle subject to the potential  $V(\mathbf{r})$ ,

$$(1) \quad i\hbar \frac{\partial \psi(\mathbf{r}, t)}{\partial t} = \left[ -\frac{\hbar^2}{2m} \nabla^2 + V(\mathbf{r}) \right] \psi(\mathbf{r}, t),$$

the separation Ansatz  $\psi(\mathbf{r}, t) = e^{-i\omega t} \phi(\mathbf{r})$  directly leads to the Helmholtz form,

$$(2) \quad [\nabla^2 + k^2 n^2(\mathbf{r})] \phi(\mathbf{r}) = 0.$$

Here,  $k = \sqrt{2mE}/\hbar$  is the vacuum wave number and  $n(\mathbf{r}) = \sqrt{1 - V(\mathbf{r})/E}$  the index of refraction. The latter depends on position and energy in the generalized case, but it reduces to unity for a vanishing potential.

To understand the elementary phenomena of matter wave optics we can thus use the concepts and the intuition gained from the study of light propagation. Static potentials can be viewed as producing the index of refraction variations required to implement lenses, gratings, and other optical elements [47]. Moreover, since the wave length  $\lambda_{dB} = 2\pi/k$  is typically much smaller than the scale of potential variations, one can usually take the short wave limit, thus switching from wave optics to ray optics when accounting for macroscopic external fields.

### 3. – De Broglie interference with clusters and large molecules

**3.1. Does size, mass or internal complexity affect the wave behavior?.** – As is well known, quantum physics is the best tested theory of nature. The concept of matter waves, which triggered its formulation, has been quantitatively confirmed with electrons, neutrons, atoms, and small molecules. One may therefore ask whether it is really necessary to further explore the wave nature of larger objects.

In fact, one can give quite a number of motivations for pursuing research in that direction. First of all, according to our everyday experience the superposition principle, which is central to quantum mechanics, does not appear to show up in our macroscopic life. For instance, we never find the position of a macroscopic object to be in a delocalized state, colloquially alluded to as ‘being in different places at the same time’. This colloquialism is actually a misnomer since position measurements have definite outcomes also in the microworld, while the delocalization can only be inferred. Yet, it remains an open and important scientific question whether quantum rules apply on all size, mass, and complexity scales.

It is therefore legitimate to ask whether there could be an objective transition between the physical laws governing the quantum and the classical world, or whether the observed

loss of quantum behavior is only a result of the fact that a complex environment is coupled to the quantum states of interest [48, 49]. This problem is also related to the question whether the unitary quantum evolution provides a complete description of all phenomena, or whether the random incidence associated with a quantum measurement process must be regarded as a fundamentally non-unitary element [50, 51]. A number of approaches try to extend quantum mechanics by relating this non-unitary element to quantum aspects of space time. Some of these proposals predict effects, which become visible in matter wave interferometry once the delocalized object exceeds a certain mass, although they agree with standard quantum mechanics at smaller masses [52, 50, 53, 54, 55, 56]. Independently of one's attitude towards such unconventional approaches, it is the genuine task of physicists to explore the practical limits of our present understanding of physical phenomena.

We have also discussed before that matter wave interferometry has found numerous practical applications, as precise 'meters' for crystal structures, surfaces or external fields. Molecule interferometry can add to that, in particular as a tool for studying *molecular properties*. This is a new perspective, related to the rich internal structure of the particle, which grows exponentially with the number of internal constituents. Also *molecular lithography* may benefit from quantum interferometry [57]. The prospects and limitations of atomic lithography as a nano-deposition technique have been discussed in [58]. Although a typical molecular beam will hardly reach the flux of the best possible atomic sources, it is worth noting that single molecules—in contrast to single atoms—can often already be regarded as functional elements by themselves. A single molecule may perform a certain task, such as acting as a logical element in molecular electronics or as a single-photon emitter in quantum optics.

Finally, interferometry with large molecules adds a plethora of new objects to the field of quantum optics. New questions and effects will arise due to their rich internal structure and nontrivial properties, which can be tailored to a large degree in the process of chemical synthesis.

Molecular quantum optics is thus an interdisciplinary endeavor, combining quantum physics, physical chemistry and the nano-sciences. It is therefore an exciting and important task to develop the molecular beam methods, coherent manipulation schemes, efficient detectors, and the tricks to avoid dephasing or decoherence for future de Broglie experiments with large molecules and supermassive clusters.

**3'2. Where is the challenge?.** – The difficulties encountered in molecule interferometry are quite substantial. They arise from the conspiracy of various hard facts, which can be summarized as follows:

- The de Broglie wavelength of an object decreases in proportion to the increase in its mass. There is nothing one can do about this scaling since we explicitly want to study very massive objects. Given the currently existing molecular beam methods and the presence of Earth's gravity one has to work with de Broglie wavelengths in the range of 10 fm to 10 pm. This is a very small length scale, ranging between

one thousandth and one millionth of the size of each interfering single cluster or molecule.

- In contrast to atoms, molecules cannot be easily controlled, slowed, or collimated by laser beams. Their rich internal structure, as well as rapid state changes on the time scale of sub-picoseconds (vibrations) and nanoseconds (electronic transitions), strongly impedes the effective external control. Over the last years, several experimental and theoretical groups have started analyzing and tackling this problem. There is, in particular, substantial progress in the handling of small molecules with switched quasi-static electric fields [59, 60, 61] and also using cavity assisted laser scattering methods [62, 63]. The controlled manipulation of large species is yet still an open challenge for several years to come.
- Atoms can nowadays be detected with an efficiency close to unity, even selectively with regard to their internal state. In contrast to that, many different detection schemes have to be explored for molecules, since each particular species responds differently to electron impact, laser excitation for fluorescence and ion collection, scanning probe techniques, and other conceivable methods.
- Interference experiments probing the coherence of matter waves must scrupulously avoid any perturbations by the environment. Complex molecules offer many additional channels for the interaction with the environment and they are therefore highly susceptible to any dephasing and decoherence effects.
- Large and thermally excited molecules often resemble small lumps of condensed matter. One consequence of this is that each individual many-body system may often be regarded as carrying along its own internal heat bath. This can determine the likelihood for exchange events between the quantum system and its environment, and thus affect the molecular coherence properties.
- Complex, floppy molecules may undergo many and very different conformational state changes even while they pass the interferometer. Several electro-magnetic properties, for instance the electric polarizability or the dipole moment, will change accordingly. This, in turn, can affect both the molecular interaction with the diffraction elements as well as their probability to couple to external perturbations.

The matter wave interference experiments with large molecules carried out in Vienna prove, in spite of all these difficulties, that quantum coherence can be generated, maintained and clearly revealed for objects composed of more than one hundred covalently bound atoms even at internal temperatures between a few hundred to 2000 K, i.e., at temperatures ten orders of magnitude beyond those required for Bose-Einstein condensation. These experiments also allow us to quantitatively investigate the influence of various decoherence mechanisms, some of which may even be used in a positive sense, for measuring molecular properties. We will describe the experiments, the required theoretical concepts, and a number of applications in the following sections.

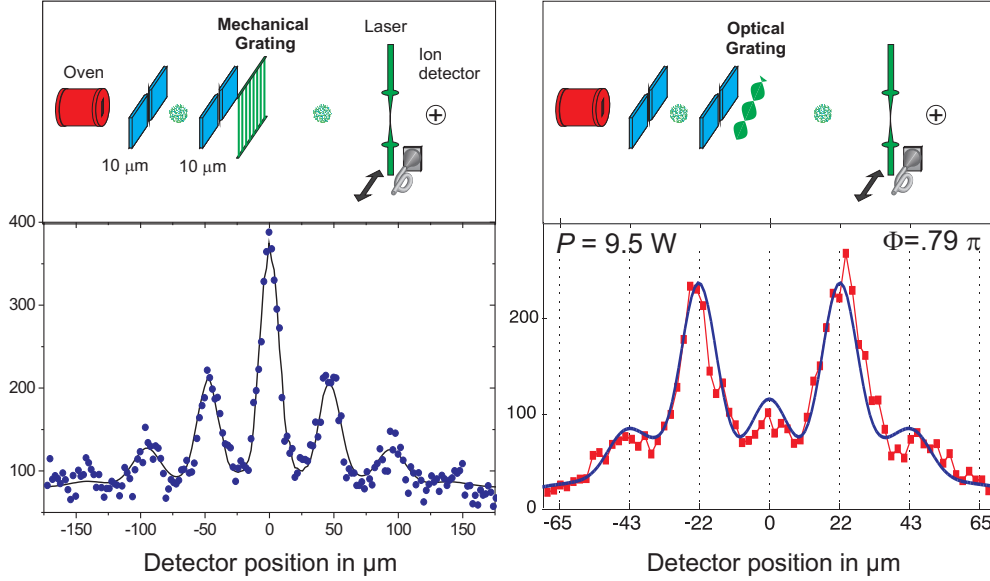


Fig. 1. – Far-field experiments with  $C_{60}$  fullerenes [64,66]. Upper left: setup for diffraction at a nanomechanical grating. Upper right: the mechanical grating is replaced by the standing light wave of a green laser beam. Bottom row: the corresponding far-field interferograms show a distinct difference in the center of the pattern [67]. Optical phase gratings are better suited for creating a wider splitting between the superposed molecular position states.

#### 4. – Quantum coherence experiments: Concepts and realizations

**4.1. Far-field diffraction of  $C_{60}$  at a nanomechanical grating.** – The coherent delocalization of large molecules was demonstrated for the first time with the fullerene  $C_{60}$ , in a far-field diffraction experiment using a nanomechanical diffraction grating made of silicon nitride. The layout of the experiment is sketched in the upper left part of Figure 1. Fullerenes can be sublimated in an oven at a temperature of 900 K. The temperature is a compromise between a sufficiently large vapor pressure and count rate on the one hand and the risk of thermal fragmentation on the other hand. An effusive molecular beam is created by a small orifice in the oven wall. At a temperature of  $T = 900$  K the most probable thermal velocity is  $v = \sqrt{2k_B T/m} = 144$  m/s, which corresponds to a de Broglie wavelength of 3.8 pm. This is already more than two orders of magnitude smaller than the size of the molecule itself.

A central issue in all interference experiments is the question of the transverse and longitudinal coherence. Since none of the molecules in the beam knows anything about the phase of the others we have to regard the molecule source in analogy to thermal sunlight. Spatial or transverse coherence is prepared by making sure that the source appears

under a sufficiently small solid angle when seen from the detector. The collimation is determined by the condition that the diffraction angle must be larger than the collimation angle. The mechanical grating in Fig. 1 has a period of 100 nm. According to textbook physics, we thus expect the first diffraction maximum at an angle of  $\theta_{\text{diff}} = 38 \mu\text{rad}$ . The collimation angle should therefore be smaller than  $20 \mu\text{rad}$ , which can be realized with two slits of  $10 \mu\text{m}$  width, separated by about 1 m.

The longitudinal coherence is determined by the velocity distribution (spectral purity) of the beam and to a good practical approximation described by the length  $L_c = \bar{\lambda}_{\text{dB}}^2 / \Delta\lambda_{\text{dB}}$ , where  $\Delta\lambda_{\text{dB}}$  is the wavelength spread around the mean value  $\bar{\lambda}_{\text{dB}}$ . A thermal molecular beam has a typical velocity and wavelength spread of  $\Delta\lambda_{\text{dB}} / \bar{\lambda}_{\text{dB}} = 60\%$ . Without any further measures, the coherence length is thus comparable to the thermal de Broglie wavelength. Using a rotating-disk velocity selector, but also using gravitational selection schemes [67] the velocity bandwidth can be narrowed down to 16 %. The coherence length is thus increased to about six times the mean de Broglie wavelength [64], which is sufficient to observe several higher diffraction orders in the far-field behind the grating, as shown on the bottom left of Fig. 1.

Fullerenes were ideal starting candidates for macromolecule interferometry since they can be prepared in high purity (better than 99%). Moreover they have many similarities to small solid state systems: At elevated temperatures they show thermal emission of electrons, comparable to the thermionic emission of a hot tungsten wire. They may emit molecular fragments, comparable to the evaporation from a solid surface. Last but not least, the photons emitted by hot fullerenes form a quasi-continuous spectrum, strongly resembling that of a black body [65].

Thermal ionization can be used in the detector stage: the molecules are irradiated with a tightly focused green laser beam which scans across the particle beam in a perpendicular orientation. The generated ions are accelerated and counted in a secondary electron multiplier as a function of the laser displacement. The result of this experiment is shown in Fig. 1. This experiment represents the first observation of quantum interference with a thermally highly excited many-body system [66, 64].

These first studies revealed already that van der Waals forces acting between the molecules and the grating walls imprint position and velocity dependent phase shifts, and thus impose stringent limits on the ability to observe matter wave interference. An indication for this fact can be obtained from a more detailed analysis of Fig. 1. As we know from our introductory optics classes, every far-field diffraction pattern of a grating with period  $d$  is modulated by an envelope given by the diffraction pattern corresponding to a single-slit. The interference maxima behind a grating are found at integer multiples of the angle  $\theta \simeq \lambda_{\text{dB}}/d$ , whereas the minima of the single-slit envelope are positioned at  $\theta \simeq \lambda_{\text{dB}}/a$ . Since our nanomechanical grating was designed with a period of  $d = 100 \text{ nm}$  and an open slit width of  $a = 50 \text{ nm}$ , the second order grating diffraction peak should therefore be completely suppressed by the single slit envelope.

The presence of the second order diffraction peak in Fig. 1 is consistent with the assumption that the attractive van der Waals interaction between the traversing molecule and the grating wall reduces the effective slit width by almost a factor of two. This huge



effect inspired experiments with optical phase gratings, where the electric field of a laser creates a dipole potential proportional to the optical polarizability of the molecule [67]. While phase gratings were already known for atoms [23], the internal molecular structure adds again to the complexity of the diffraction physics, since the molecular line widths can be as broad as 30 nm to 50 nm at elevated temperatures. The electromagnetic field therefore does not induce virtual transitions corresponding to a single, spectrally sharp atomic line, but rather acts on the far-detuned wings of all molecular resonances, where the optical polarizability approaches the static polarizability.

**4.2. Molecular far-field diffraction at a standing light grating.** – Figure 1 shows on the right-hand side the experimental configuration where a retro-reflected focused Argon ion laser beam (with a wavelength of  $\lambda_L = 514$  nm) forms a phase grating with a period of 257 nm for the passing  $C_{60}$  molecules. The far-field diffraction pattern presented in the lower right panel of Fig. 1 is in very good agreement with the theoretical expectation.

Such phase gratings of light have several distinct advantages over nano-fabricated structures: Even lasers with a moderate bandwidth produce nearly perfect periodic gratings which neither clog nor break. An additional knob is offered in the experiment by the possibility to vary the laser intensity, and the problem of van der Waals forces is eliminated at the expense of somewhat increased alignment requirements. A new aspect is the possibility of photon absorption, although the absorption cross section is sufficiently small in the case of  $C_{60}$  to be negligible for the experiments.

However, interference fringes can be observed also for  $C_{70}$  fullerenes, where the cross section is larger by almost an order of magnitude, so that on average one photon is absorbed during the molecular passage through the grating. This highlights a peculiarity of large molecules: After absorbing a photon they preferentially channel the photonic energy into vibrational excitations rather than in re-emitting fluorescent light. This intra-molecular energy increase occurs coherently at all positions within the standing light grating, so that the internal and the motional states of the molecule remain separable. At the same time, the absorption of a single photon changes the transverse momentum of the molecule by  $h/\lambda_L$ . The associated far-field probability distribution then gets shifted by exactly half a period, which blurs the fringe pattern. In contrast, the absorption of two photons hardly affects the visibility because it shifts by a full period (or not at all if the photon momenta have opposite momentum). Since the probability for absorbing no or two photons is always greater than the likelihood of a single photon absorption, a fringe pattern can still be observed. This is different to the effect of photon scattering in atom interferometry experiments [68, 39], where the photon may be scattered in all directions, thus blurring the interference fringes very efficiently.

## 5. – Near-field interferometers for massive molecules

Observing a far-field diffraction pattern behind a material grating probably constitutes the most direct prove of the wave-nature of matter. However, as discussed above, this requires the preparation of sufficient coherence, which in turn is based on the tight

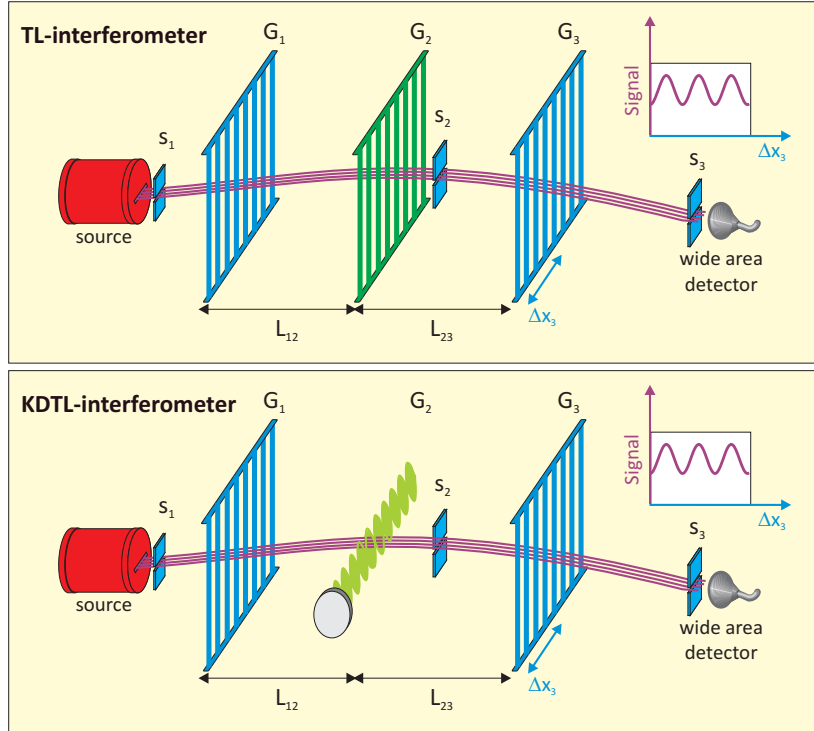


Fig. 2. – Setup of the mechanical Talbot-Lau interferometer (top) and the Kapitza-Dirac-Talbot-Lau interferometer (bottom). Top: The gratings in the TLI are made of gold, with a period of about  $1\mu\text{m}$ , separated equidistantly by a distance between 22 cm and 38 cm, which corresponds to one or two Talbot lengths, depending on the molecular velocity. Bottom: The first and third grating in the KDTLI are made of a 190 nm-thick silicon nitride membrane with a grating period of 257 nm. This corresponds to half of the wave length of the laser beam, which is used to create a standing light wave by retroreflection. In the experiment it is crucial that the periods of the mechanical and the light gratings match exactly, already a deviation of  $0.5\text{\AA}$  would substantially reduce the fringe visibility.

collimation of the incident incoherent molecular beam. Molecules which are even more massive than the fullerenes will give rise to smaller diffraction angles and, correspondingly, they will require even tighter collimation angles. We thus encounter a very natural practical limitation for this type of experiments below a de Broglie wavelength of around 1 pm. In combination with the 100 nm sized diffraction structures, such waves interfere constructively at angles close to  $10\mu\text{rad}$ . The preparation of coherence would thus require the molecular beam to be collimated below a few microradians, which borders on the technologically possible. Of course, smaller grating structures would yield wider diffraction angles, but the aforementioned influence of van der Waals forces and, ultimately, the lateral dimensions of large molecules set here strict limits, too.

In order to demonstrate the wave nature of massive molecules it is therefore highly desirable to work with wide grating openings and less demanding collimation requirements. The solution is found in near-field interferometry, which can be implemented in analogy to the optical counterparts discussed by H. F. Talbot [69] and E. Lau [70]. This idea was first implemented for atoms [71], and also suggested for high-mass experiments [72] by J. Clauser. The first near-field interferometer for molecules was then realized in our group in Vienna in 2002 [73].

The Talbot effect is a coherent self-imaging phenomenon. It describes the fact that a plane wave traversing a periodic absorptive structure will image this structure in integer multiples of the Talbot distance  $L_T = d^2/\lambda_{\text{dB}}$  by virtue of the resonant near-field interference of different diffraction orders [69]. Remarkably, the coherent self-imaging can be employed even for spatially incoherent sources if one adds a second grating, as shown in Fig. 2. In this arrangement, each slit in the first grating may be viewed as selecting an elementary spherical Huygens wavelet, which propagates towards the second grating, thus creating the required coherence. If the de Broglie wavelength meets the Talbot resonance criterion, an interference pattern appears behind the second grating as an overlay of all the single self-images originating from the individual slits of the first grating. In the simplest case, where the distance  $L_{12}$  between the first and the second grating equals the distance  $L_{23}$  between the second grating and the detection plane, the image emerging in the plane of the third grating shows the highest visibility provided that the period of the array of slit sources  $G_1$  equals the period of the second grating  $G_2$ . In contrast to the pure Talbot effect, where self-imaging occurs precisely at integer multiples of the Talbot-distance, the Talbot-Lau contrast may be quite small at exactly this distance but it rapidly increases in the neighborhood if the grating separation is symmetrically stretched or compressed [73,74].

There are many ways to detect the Talbot-Lau interferogram in the plane  $G_3$ . A method that combines high spatial resolution with high detection efficiency places a third grating in the image plane, as indicated in Fig. 2. The latter has the same period as the interferogram so that the transmitted molecular flux gets modulated in its intensity if we vary the transverse position  $x_s$  of the third grating. Plotting the total molecular intensity  $S(x_s)$  behind the third grating as a function of its position  $x_s$ , directly reveals the interference pattern. This 3-grating arrangement is designated as a Talbot-Lau interferometer. The first molecule interferometer exploiting this principle was made from three gold gratings with a period of 990 nm [73]. Figure 3 presents a typical interferogram, recorded for the molecule tetraphenylporphyrin displayed in Fig. 5.

For our typical experimental conditions the interference pattern is well described by a sine curve, whose period is given by the diffracting structure. Such a periodic curve is readily characterized by its contrast or visibility, defined in terms of the maximum and minimum count rates as

$$V = \frac{S_{\text{max}} - S_{\text{min}}}{S_{\text{max}} + S_{\text{min}}}.$$

If the signal varies by a factor of two, as is roughly the case in Fig. 3, its fringe visibility

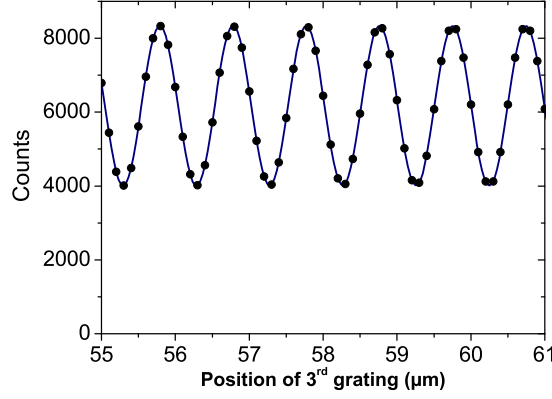


Fig. 3. – Typical molecular density pattern at the exit of a Talbot-Lau interferometer. The fringe period of 990 nm is determined by the period of the nanomachined grating. It is therefore independent of the de Broglie wavelength. The fringe visibility, however, is strongly dependent on the de Broglie wavelength, which is set by choosing the beam velocity, see Fig. 4.

amounts to  $V=33\%$ . We can now use the fringe contrast to clearly distinguish genuine quantum interference from a classical moiré-type shadow image, which might also result from the classical flight of point particles through a sequence of two or more gratings. As shown in Fig. 4, the velocity dependence (i.e., wavelength dependence) of the quantum fringe visibility differs both quantitatively and qualitatively from all classical predictions.

A detailed analysis [74, 75] must again include the influence of van der Waals forces between the molecules and the grating walls. It turns out that the effect of this dispersive interaction is much stronger than in far-field interference. This can be seen in Fig. 4, where the dashed line gives the quantum wave prediction for Talbot-Lau interference of  $C_{70}$  if we disregard the existence of van der Waals forces. The experimental observation differs qualitatively, and only by accounting for the dispersive interaction we obtain a good quantitative agreement with the experimental observation [73], as represented by the solid line. An even better agreement is obtained in the high velocity wing if the Casimir Polder potential, i.e. the fully retarded version of the interaction is used (not shown here).

The Talbot-Lau interferometer was applied to demonstrate the wave-like behavior of particles as massive as  $C_{60}F_{48}$ , cf Fig. 5b, which comprises already more than one hundred atoms in a round compound of 1632 amu [76]. In the same setup we observed high-contrast interference fringes of tetraphenylporphyrin  $C_{44}H_{30}N_4$  [76], an extended and strongly oblate biodye, which is a relative to the color centers in hemoglobine and chlorophyll, see Fig. 5c.

Attempts to go to even larger molecules in this particular experiment are impeded

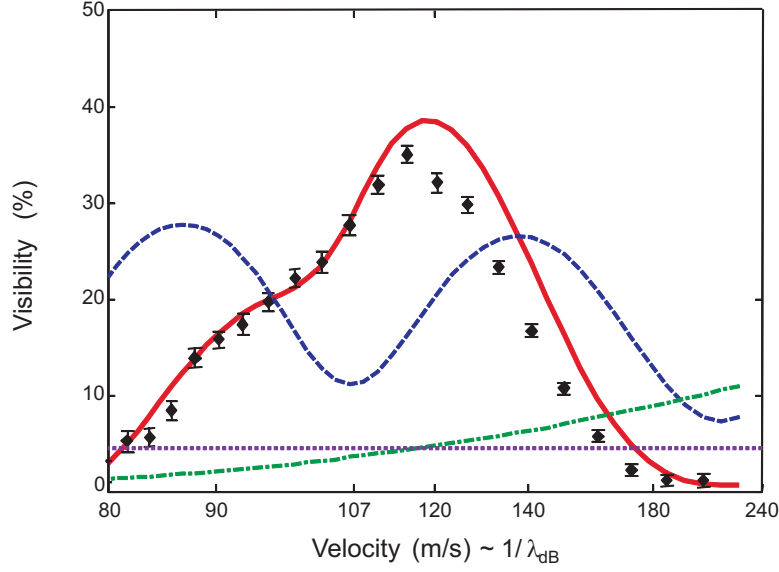


Fig. 4. – Dependence of the fringe visibility of  $C_{70}$  interferograms on the de Broglie wave length, as characterized by the mean beam velocity. The full diamonds give the experimental result obtained in a mechanical TL-interferometer, with a molecular velocity spread  $\Delta v/\bar{v}$  ranging from 8% to 35% at the large mean velocities [73]. The theoretical curves account for this distribution of wavelengths in the beam. The dashed line gives the quantum mechanical expectation, assuming that the molecules are ideal point particles which do not interact with the grating walls. A good agreement with the experimental observation is only obtained by accounting for the forces exerted on the polarizable molecules due to the van der Waals interaction with the grating walls (solid line). The discrepancy at high velocity is reduced if one includes the effects of retardation as described by the Casimir-Polder potential. The bottom lines are the result of a classical calculation assuming that the molecules follow Newtonian trajectories. Unlike the dotted line, the dash-dotted one includes the van der Waals forces. One observes that only the quantum mechanical calculation is able to describe the experimental data.

by the increasingly strong effect of the dispersive interaction with the grating walls [78]. For molecules with a similar composition, the electric polarizability increases with the particle size, and also the grating interaction time increases with the mass, since smaller velocities are required to keep the diffraction angles and thus the Talbot length constant. The grating interaction thus imposes increasingly strict requirements on the longitudinal coherence in the molecular beam, which becomes rather demanding beyond masses of 1000 amu.

In order to circumvent these dispersive interaction effects, we replaced the central material grating by an optical phase grating, as shown in the lower panel of Fig. 2. We call this setup a Kapitza-Dirac-Talbot-Lau interferometer [78], since it combines the idea of coherent self-imaging, as present in the Talbot-Lau concept, with diffraction of matter at standing laser light gratings, as originally proposed by Kapitza and Dirac for the

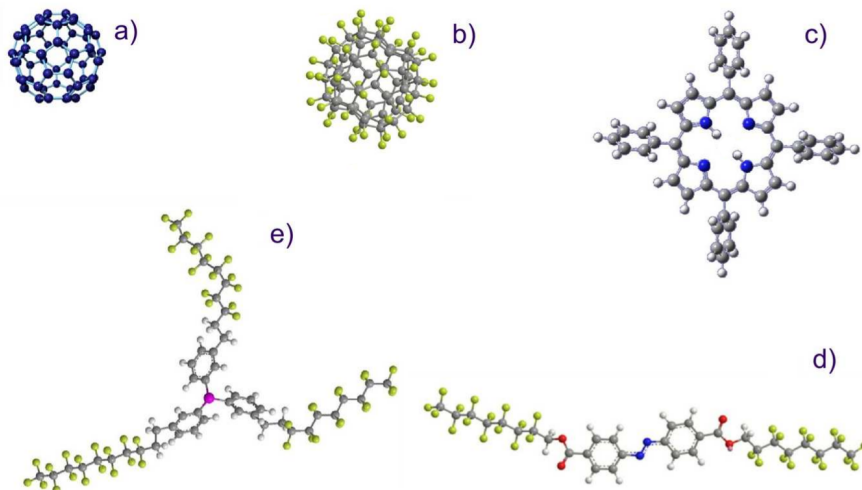


Fig. 5. – Gallery of molecules that revealed their quantum nature in the Viennese Talbot-Lau setup and in the Kapitza-Dirac-Talbot-Lau interferometer. The relative size of the molecules is roughly to scale. a)  $C_{60}$  buckyball [66]. b) fluorinated fullerene  $C_{60}F_{48}$  [76]. c) Tetraphenylporphyrin  $C_{44}H_{30}N_4$  [76]. d) perfluoroalkyl-functionalized diazobenzene  $C_{30}H_{12}F_{30}N_2O_4$  [78]. e)  $C_{48}H_{24}F_{51}P$ , a fluorinated catalyst molecule [77].

diffraction of electrons [79]. The phase shift imprinted by the standing light wave can be easily adjusted by the laser power.

Using the the Kapitza-Dirac-Talbot-Lau interferometer we demonstrated the wave nature of perfluoroalkyl-functionalized azobenzene molecules [78]. These polyatomic molecular chains have a length of 32 Å. In their stretched trans-conformation they are four times more extended than the fullerene  $C_{60}$ . In comparison to the soccer ball shaped fullerenes, the azobenzene derivatives rather resemble strings, and numerical simulations [80] confirm that they undergo lively configurational state changes on a time scale shorter than the passage time through the interferometer. In spite of that complicated internal dynamics, they produce interference fringes with a contrast which is in full quantitative agreement with a quantum calculation based on its molecular mass and static scalar polarizability. Similarly, we observed undiminished interference of  $C_{48}H_{24}F_{51}P$ , a fluorinated catalyst molecule with a mass of 1600 amu which is comparable to  $C_{60}F_{48}$ , but significantly more extended [77]; its three-legged configuration is shown in Fig. 5e.

## 6. – Decoherence and dephasing in matter wave interferometry

**6.1. The concept of decoherence.** – The experiments described so far clearly indicate that even large and complex molecules can exist in the delocalized state required for interference at a grating. This is quite remarkable since such molecules are usually

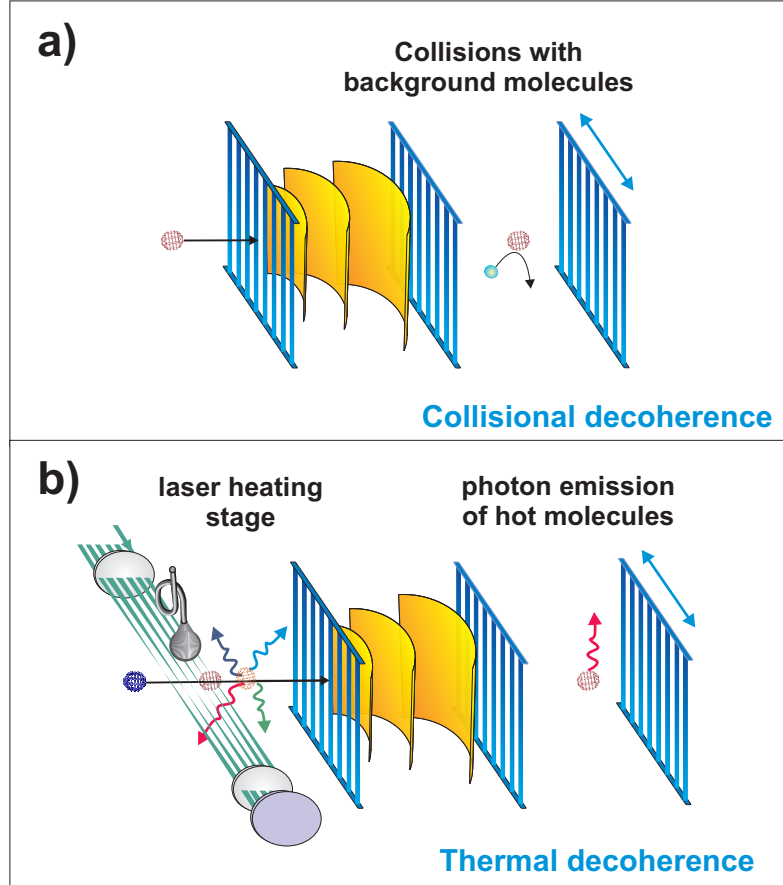


Fig. 6. – Decoherence is a consequence of the coupling of the quantum system to a practically uncontrollable environment. In our experiments we studied (a) the effect of collisions with residual background gases [84] and (b) the localization of hot fullerenes through emission of heat radiation [85, 86].

viewed as well-localized objects that we can even observe in high-resolution microscopy.

From a quantum mechanical perspective, this apparent emergence of classicality, namely how and when an object loses its quantum features and becomes indistinguishable from a classical description, can be explained to a large extent by decoherence theory [81, 82, 83]. The crucial point is to acknowledge that no quantum object is completely isolated. It is embedded in an environment consisting of gas particles, photons and the like. Since the environmental state gets very quickly correlated due to quantum interactions with the object, information about the whereabouts of the quantum object is

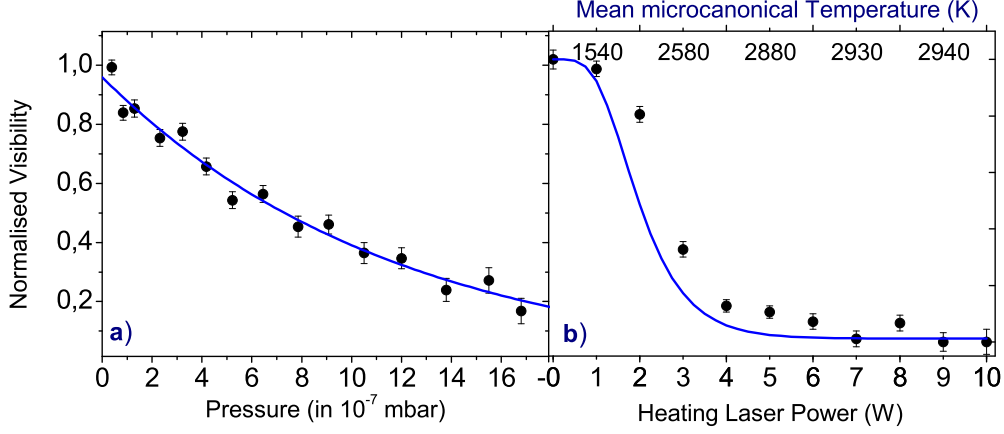


Fig. 7. – Left: Collisional decoherence leads to an exponential decay of the fringe visibility with increasing residual gas (methane) pressure [84]. This observation is in good agreement with the scattering theory calculation (solid line). Right: Heating the fullerenes with a laser prior to entering the interferometer leads to a non-exponential decay of the interference visibility. It is quantitatively explained by the heat radiation due to the molecular temperature (upper scale), which in turn is extracted from the heating dependence of the detection efficiency [85, 74].

rapidly disseminated into the surroundings. An initially pure state of the molecule is thus quickly replaced by a mixed one, once the environmental state is disregarded due to its practical inaccessibility. The absence of quantum behavior in the macroworld is then a natural consequence of the fact that bigger and more complex objects are much harder to isolate. The particular features of the environmental interaction and the resulting transfer of which-path information thus lead to the emergence of classical behavior in the motion of mesoscopic quantum objects.

What are possible effects that might destroy a molecule's coherent, delocalized state? One can conceive all sorts of scattering processes with massive particles and light, originating from local sources such as residual background gases and thermal photons up to neutrinos and cosmic radiation. In our experiments, there are at least two relevant and ubiquitous mechanisms that serve to effectively measure the position of a molecule. The first is due to collisions with background gas molecules, while the second involves radiation emitted by the thermally excited diffracting molecules.

**6.2. Collisional decoherence.** – To find out how the interaction with a background gas can destroy the interference pattern and lead to classical behavior, we gradually added various gases to the vacuum chamber of our Talbot-Lau interferometer during the experiments with  $C_{70}$  fullerene molecules, see Fig. 6a. We found that the amount of contrast between the interference fringes fell exponentially as more gas was added, and that the fringes disappeared almost entirely when the pressure had reached just



$10^{-6}$  mbar [84]. This can be seen in Fig. 7a for the case of methane gas. In fact, this observation is in full quantitative agreement with a theoretical analysis of the scattering processes [87, 88]. Although a single collision with a gas molecule will not kick the massive fullerene out of the interferometer path, it is enough to destroy the interference pattern. The effect can be explained by the momentum exchange experienced, or equivalently, by the fact that the scattered gas particle carries sufficient information to determine the path that the interfering molecule has taken.

Since the gas particles at room temperature have large velocities, centered around  $\tilde{v}_g = \sqrt{2k_B T/m_g}$ , it is justified to assume that a beam molecule gets completely localized by a single collision. The exponential decay is thus directly related to the collision probability, described by the thermally averaged, effective cross section [84, 88, 89]

$$\sigma_{\text{eff}}(v_m) = \frac{4\pi\Gamma(9/10)}{5\sin(\pi/5)} \left( \frac{3\pi C_6}{2\hbar} \right)^{2/5} \frac{\tilde{v}_g^{3/5}}{v_m} \left[ 1 + \frac{1}{5} \left( \frac{v_m}{\tilde{v}_g} \right)^2 \right].$$

Here,  $v_m$  is the velocity of the beam molecules, the constant  $C_6$  describes the van der Waals potential  $U(r) = -C_6/r^6$  between molecule and gas particle, and  $\Gamma$  denotes the Gamma function. For a TLI with gratings equally separated by the distance  $L$  the suppression of the visibility at gas pressure  $p_g$  is then given by

$$\frac{V(p)}{V_0} = \exp \left( -\frac{2L\sigma_{\text{eff}}(v_m)}{k_B T} p_g \right).$$

The observed contrast reduction was in good agreement with this formula for the various gases we investigated, see Fig. 7a. Our calculations suggest that molecules as massive as  $10^6$  amu would still be unaffected by collisional decoherence in a realistic Talbot-Lau interferometer, provided the pressure does not exceed  $10^{-10}$  mbar, which is not trivial but certainly feasible with existing vacuum technologies.

We note that the concept of an index of refraction, which was discussed in Sect. 2 can be extended to the case where a background gas acts as a medium for the matter waves. One cannot describe collisional decoherence this way, but it may still be used to account for the coherent modification due to the background medium, as well as for the dampening of the beam due to collisions leading to a complete loss. This gas-induced index of refraction  $n$  is determined by the forward scattering amplitude  $f_0$  as  $n = 1 + \hbar^2 \pi n_{\text{gas}}(\mathbf{r}) \langle f_0 \rangle / (m_* E)$ , with  $n_{\text{gas}}(\mathbf{r})$  the local gas density and  $m_*$  the reduced mass; it involves an appropriate averaging over the thermal velocity distribution in the gas [90, 91]. According to the optical theorem  $f_0$  has an imaginary part determined by the total scattering cross section. It renders  $n$  complex and thus describes the dampening of the matter wave beam due to collisional losses. The phase shifts and losses described by this index of refraction have recently been measured with an atomic Mach-Zehnder interferometer [36, 92].

**6.3. Thermal decoherence.** – We now ask how the ‘internal temperature’ of a molecule affects its ability to interfere. The concept of an internal temperature is not particu-

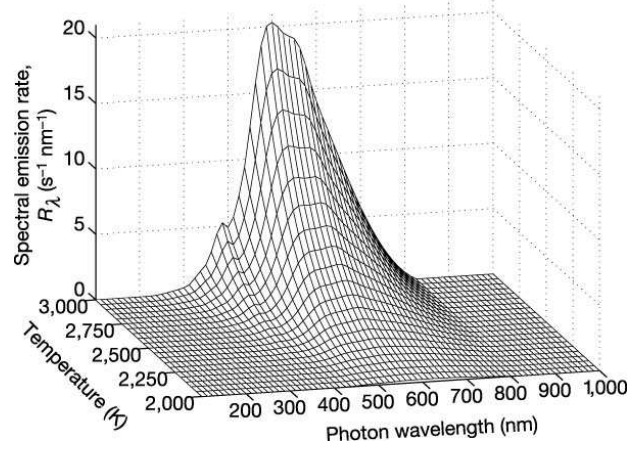


Fig. 8. – Spectral photon emission rate of  $\text{C}_{70}$  fullerenes as a function of their internal (microcanonical) temperature [85]. It is used to calculate the decohering effect of thermal heat radiation. The suppression of long wave length photons is due to the electronic excitation gap in  $\text{C}_{70}$  of about 1.5 eV.

larly meaningful for atoms, not to speak of elementary particles. However, for complex objects such as large molecules it is very natural to describe the energy distribution of the many vibrational and rotational degrees of freedom in terms of the micro-canonical temperature.

This applies in particular to fullerenes, which are very stable and which are able to store energies corresponding to an internal temperature of up to 5000 K before they start decomposing in free flight. Heating can be done using intense visible laser light. Each green photon of an Argon ion laser (514 nm) increases the average internal temperature by about 170 K and the setup allowed to deposit up to about 50 photons per molecule.

Hot fullerenes are known to emit heat radiation in a continuous spectrum similar to a black body [65]. One must, however, account for the frequency dependence of the emission cross section, rendering fullerenes 'grey' rather than black bodies. In addition, their finite heat capacity plays a role as well as the fact that the emission is not in thermal equilibrium with the external thermal radiation field [93]. Also, competitive processes such as electron and  $\text{C}_2$  fragment emission have to be taken into account.

Based on a correspondingly adapted version of Planck's law, which involves the measured frequency dependent absorption cross section, one can describe the spectral photonic emission rate  $R_\lambda$  as a function of the internal molecular temperature, see Fig. 8. According to decoherence theory, all it takes to destroy the interference fringes is for the molecule to emit either lots of long-wavelength photons or a single photon with a wavelength shorter than about twice the separation between the coherently split molecular wavelets.

This can be seen from the formula for the visibility suppression, which involves an

integration over all photon wavelengths  $\lambda$  and over all longitudinal positions  $z$  in the interferometer [85, 93],

$$\frac{V(T)}{V_0} = \exp \left[ - \int_0^{2L} \frac{dz}{v_z} \int_0^\infty d\lambda R_\lambda(\lambda, T) \left\{ 1 - \operatorname{sinc} \left( 2\pi \frac{d}{\lambda} \frac{L - |z - L|}{L_T} \right) \right\} \right].$$

At each position  $z$  the argument of the function  $\operatorname{sinc}(x) = \sin(x)/x$  compares the photon wavelength to the effective path separation, which varies (for  $L = L_T$ ) between 0 and the grating period  $d$ . Whenever the photon wavelength can ‘resolve’ this path separation, which is largest at the second grating, the sinc function is substantially smaller than unity and thus should give rise to a suppressed visibility.

Indeed, when we increased the internal temperature of  $C_{70}$  fullerene molecules to above 1000 K, the contrast between the interference fringes slowly disappeared, see Fig. 7b [85]. In the experiment we varied the temperature by heating the molecular beam in front of the interferometer with a crossing laser beam, as shown in Fig. 6b. Our understanding of the beam temperature and its cooling dynamics was independently checked by recording the heating dependence of the detection efficiency at various beam velocities [93]. Using this temperature variation as an input to our microscopic decoherence model the observed decoherence rates were reproduced quantitatively, as can be seen by the solid line in Fig. 7b. This good agreement between the predicted and the measured decoherence rate indicates that the  $C_{70}$  molecules emitted a few visible photons (with a broad band of wave lengths centered around 800 nm) when they were heated to internal temperatures above 2500 K. Since the grating slit separation was  $1 \mu\text{m}$ , this sufficed to substantially reduce the fringe visibility, as enough ‘which-path’ information became available to the environment.

This experiment proves that decoherence due to heat radiation can be quantitatively traced and understood. It confirms the view that decoherence is caused by the flow of information into the environment, mediated by a transfer of momentum. Finally, it shows that thermal decoherence is very relevant for mesoscopic and macroscopic objects. Large molecules are already sufficiently complex to serve as their own internal heat bath, leading to auto-decoherence, provided they are sufficiently hot. In that sense, they can be regarded as condensed matter systems.

Fortunately, this effect will be less of a concern in future interferometry experiments with large molecules, clusters or nanocrystals. Objects like these will have to be substantially cooled in their external degrees of freedom, to make them coherent in the first place. All cryogenic cooling methods will have to additionally reduce the internal temperature and thus the probability for the emission of thermal radiation.

**6.4. Dephasing and phase averaging.** – In addition to the proper decoherence mechanisms mentioned above, we have to deal with a number of other issues that do not involve the quantum interaction with the environment, but which may still significantly affect the interference quality. In practice, these phenomena are hard to distinguish from genuine decoherence, even though their theoretical description is rather different.

A simple, yet very relevant effect is the phase averaging brought about by acoustic vibrations of the interferometer. Due to these vibrations subsequent molecules 'see' the gratings at slightly different spatial locations, so that each interfering molecule gives rise to a probability distribution that is out of phase with respect to a previous one. The resulting blurring of the observed interference pattern can be quite strong [94]. At certain frequencies vibration amplitudes as small as 15 nm can be detrimental, even if the grating constant is as wide as 1  $\mu$ m. This finding imposes severe constraints on the allowed vibration amplitudes for all future experiments, which will inevitably have to work at even smaller grating constants. A related issue is the thermal drift in the interferometer apparatus, which must be eliminated or controlled with a similar degree of accuracy.

Another, equally coherent effect, that may affect the interference contrast, is due to the fictitious forces brought about by the fact that the laboratory is not an inertial system. In the laboratory frame the molecules are accelerated by the gravitational field and they experience a Coriolis force due to Earth's rotation. Matter wave interferometers are very sensitive to these effects, and in fact, atom interferometers are currently among the best devices for measuring the corresponding accelerations [29, 34, 32].

If the molecular beam was monochromatic there would be no reduction of visibility, only a shift of the pattern due to the non-inertial forces. However, this shift is at least inversely proportional to the beam velocity [94]. Even though the interferometer would accept a rather broad velocity distribution if it was at rest in an inertial system, the fictitious forces now introduce a strong dispersion by shifting the interference pattern to different positions for different velocity components. This introduces again an effective blurring of the interference signal which is aggravated for increasingly massive particles with small beam velocities.

In particular, in case of a constant acceleration  $a$  the interference contrast gets reduced by

$$\frac{V}{V_0} = \exp \left( -2 \left[ \pi \frac{aL^2\sigma_v}{dv_z^3} \right]^2 \right)$$

where  $d$  is the grating period,  $v_z$  is the longitudinal velocity,  $\sigma_v$  its spread, and  $L$  is the grating separation. In the case of gravity, we can substitute  $a = g \sin \theta$ , where  $\theta$  gives the tilt of the interferometer plane with regard to the local direction of the gravitational acceleration. For the Coriolis force we may substitute  $a = 2v\Omega_0 \cos \phi$ , where  $\phi$  is the angle between the normal on the interferometer plane and the rotation axis of the earth, spinning at angular frequency  $\Omega_0$ .

## 7. – Matter wave interferometry for molecule metrology

Let us now turn to the question how the interference of molecules can be used to measure molecular properties. A first application, which was demonstrated recently, is the measurements of the static and the dynamic polarizability of large molecules [95, 96].

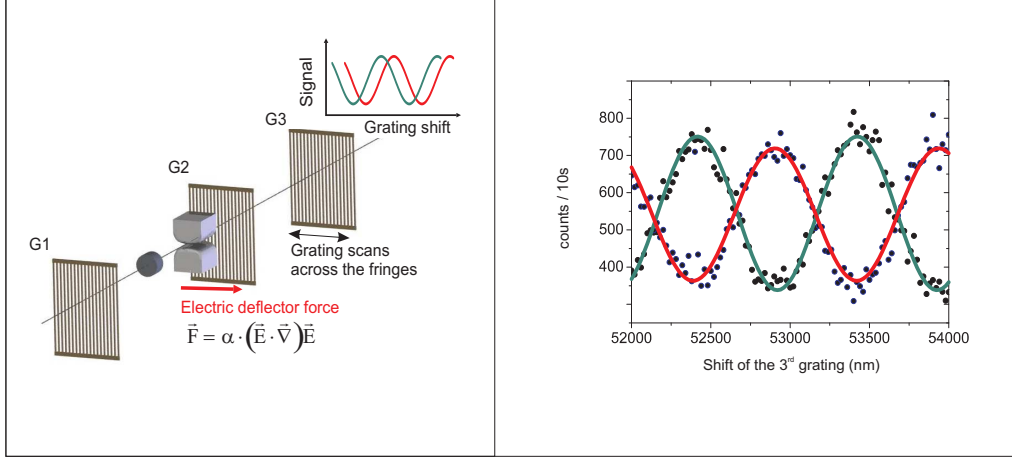


Fig. 9. – left: Setup for interferometric deflectometry. The traversing clusters and molecules interact with both the optical phase grating and the electric field gradient via their polarizability and/or electric dipole moment. Generalizations to measurements of magnetic moments and magnetic susceptibilities are well conceivable. right: The fringe shift of the molecular interferogram in the external electric field permits to directly determine the molecular polarizability with high precision. This curve was obtained with three mechanical gratings, i.e., in the Talbot Lau setup [95].

In contrast to earlier atom interferometric polarization measurements [97], the Talbot-Lau concept does not allow one to address two individual interference paths separately. However, the gratings imprint a nanostructure onto the molecular beam, which admits the measurement of tiny beam shifts with high precision. At the same time, the interaction between the flying molecules and both the material and the optical gratings depends sensitively on the electric polarizability, or more generally the electric susceptibility, which also includes the molecular permanent electric dipole moments.

The experiment shown in Fig. 9 depicts a Talbot-Lau interferometer into which a specifically designed deflection electrode was inserted [98]. The electrode is designed to provide a most homogeneous electric force field  $F = \alpha(\vec{E}\vec{\nabla})\vec{E}$  over the cross section of the laterally extended molecular beam. This leads to a molecular beam deflection at the location of the third grating proportional to

$$x_d \propto \frac{\alpha}{m} \frac{(\vec{E}\vec{\nabla})\vec{E}}{v_z^2}.$$

When we vary the voltage  $U$ , and thus the electric field  $E$  across the electrodes, we find a shift of the molecular interference pattern. By fitting a parabola to the data we can extract the polarizability with an accuracy of currently about 4 percent. This good degree of precision results from the high resolution of the fringe shift of 10...15 nm, and

from the velocity spread in the present beam configuration, which amounts to about 15%.

These parameters can certainly still be improved. Future deflectometer measurements will clearly profit from molecular beams with narrower velocity bands. On the other hand, it is worth noting that even at the present resolution interesting statements can be made about the internal molecular state. Molecules of identical mass and composition may have dramatically different structures and conformations giving rise to strongly different electrical response functions. This is the case, in particular, for sequence isomers of polypeptides and for conformation isomers of azobenzene derivatives or retinal. Similarly, metal clusters of the same mass may be in different magnetic states. It is thus conceivable to analyze such isomers, and even to sort mixtures of them, by using a Talbot Lau interferometer [99].

The Kapitza-Dirac-Talbot-Lau interferometer described in Sect. 5 offers the possibility to also measure the *optical* polarizability at the frequency of the standing light field [96]. One records the interference visibility as a function of the laser power and the mean velocity in the beam. By fitting the results of the quantum calculation to these data, one can extract the complex dynamic polarizability with good accuracy, similar to the mentioned deflection experiment.

One may also think of combining the deflectometry scheme with the Kapitza-Dirac-Talbot-Lau interferometer. This way the contribution of permanent electric dipole moments could be accessed, since the optical field changes its sign at a frequency way too fast for the dipoles to follow, while the static field may orient them. A KDTLI-deflectometer thus opens the possibility to measure the static susceptibility and the optical polarizability at the same time. A direct comparison should then allow one to separate the influence of polarizability and static dipole moments and to determine them independently with good accuracy in future experiments.

These investigations will become increasingly relevant as new methods are being developed to cool the internal molecular states as well. Molecule interferometry may then become an interesting add-on to mass spectrometry [77].

## 8. – Optical imaging of sub-wavelength molecular nano-interferograms

In the previous chapters we focused primarily on the methods required to prepare and maintain coherence, and to use it in interferometric measurements. However, daily life in the lab is also strongly concerned with the preparation of sufficiently intense molecular beams, and with methods to efficiently detect the slow, neutral molecules.

It is beyond the scope of this contribution to summarize all methods that were explored and developed in the context of our Vienna experiments on molecule interferometry. One example seems particularly instructive, though, and useful also in future experiments. It is the mechanical magnification of surface-recorded molecular interferograms, which serves as an alternative detection scheme.

The ionization of organic molecules with masses beyond a few thousand amu is generally considered to be a big challenge. Often the ionization energies are too high to be

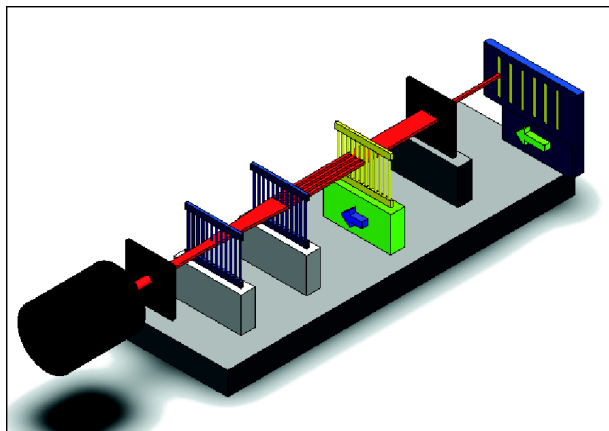


Fig. 10. – Setup for mechanically magnified imaging of a near-field molecular interferogram. The Talbot-Lau interferometer transmits a molecular beam over a restricted lateral width of about  $100\ \mu\text{m}$ . This beam is collected on a quartz surface after mechanical magnification as described in the text. The longitudinal velocity is encoded in the falling height, i.e., the  $y$ -position of the molecular beam on the screen. The position of the third grating is encoded in the  $x$ -position of the comoving quartz plate [100].

accessible with available laser light, or neutral fragmentation is energetically favored [101]. Efficient photo detection of neutral organic clusters is therefore only possible in selected cases, such as for  $\text{Trp}_{30}\text{Ca}$  [102].

On the other hand, large organic molecules often fluoresce quite efficiently. Even if they cannot do this natively they can be labeled with fluorescent dye tags. In this sense, fluorescence detection gets increasingly simple for large molecules. One might therefore consider the direct optical imaging of interferograms. An obvious problem with this is that the quantum interference fringes of high-mass molecules will generally be rather narrow, in fact often below Abbé's optical diffraction limit  $a \simeq \lambda/2$ .

A simple, yet very efficient approach to the imaging of periodic sub-wavelength molecular structures is the use of mechanical magnification. In the experiment we enlarge the interference pattern by about 1:4000 in order to facilitate the imaging of the interferogram. An illustration of the setup, shown in Fig. 10, explains the idea: we place a transparent recording quartz plate behind the mechanical TLI and thus collect all molecules that pass the interferometer. The counting of the plate-deposited molecules serves only one purpose: measuring the transmitted molecular flux. It may in addition happen that a fine-grained molecular interference pattern also forms on the quartz plate if the plate is positioned in the proper distance behind the third grating. However, we do not use this information. In the end we only record the total fluorescent light, which is proportional to the integrated number of transmitted molecules, as long as the deposited layer is sufficiently thin.

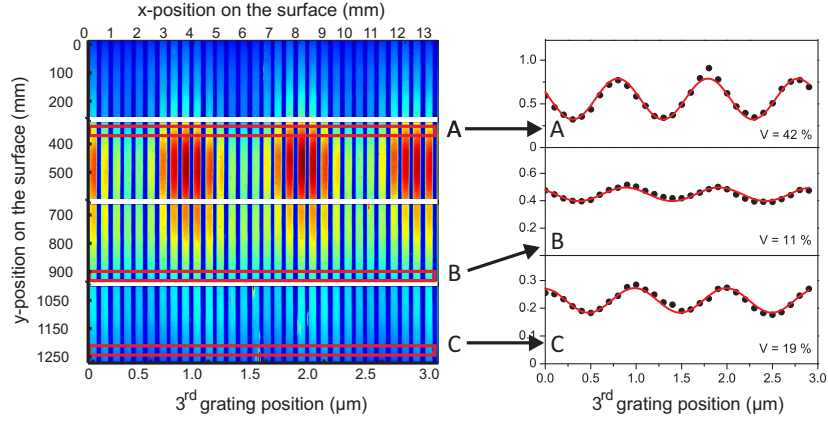


Fig. 11. – Left: Fluorescence microscopy image of a porphyrin interferogram with mechanical magnification. One clearly observes interference patterns of different contrast for different molecular velocities. Right: A trace along three selected vertical positions reveals the interference fringe more clearly [94].

The interference information is now magnified and encoded by scanning the third grating across the molecular density pattern as in the Talbot-Lau experiments described in Sect. 5. For each discrete scan position of the third grating (step size 100 nm) the quartz plate is moved by a significantly larger distance, for instance 400  $\mu\text{m}$ , corresponding to a 4000-fold mechanical magnification. The resulting large area molecular deposit can then be read in fluorescence microscopy. The result of this is presented in Fig. 11. The abscissa encodes the transverse position of the third grating, while the ordinate encodes the vertical position of the molecules in the lab frame. Here we explicitly make use of a gravitational velocity selection scheme [67]. It exploits that slow molecules have a longer time of flight. They fall deeper and thus arrive lower on the plate than the fast molecules. The optical recording thus permits us to directly reveal the functional relation between the fringe visibility and the molecular de Broglie wavelength (velocity), as shown in Fig. 11b.

This trick of optically imaging sub-wavelength molecular interferograms by means of mechanical magnification is a scalable method. It may be applied to particles of any mass, as long as they fit through the grating slits and as long as they can be marked by fluorescent dyes.

## 9. – The future of quantum experiments with clusters and molecules

Our experience in the realm of quantum experiments with complex compounds taught us that sizable challenges are piling up if one tries to increase the mass, size and complexity of the interfering object. At the same time, many interesting avenues are opening up:



On the one hand, it remains an important goal to explore the ultimate mass limit of quantum interferometry. This is a worthy and thrilling experimental challenge in itself. In addition, as mentioned in Sect. 3, various theoretical proposals have emerged in recent years, some of them still in a rather early stage of formal justification, that suggest that fundamental effects might suppress the visibility of quantum interference beyond a certain mass limit. This implies the experimentally appealing perspective, that the persistence of quantum interference beyond a certain mass and coherence time may allow us to test and potentially falsify certain unconventional extensions of quantum mechanics and theories of quantized space time. The current range of parameters is so wide that some models start being touched by our current experiments, while others still lie in the future by six to seven orders of magnitude in mass. That is pretty far—but not beyond the means of feasibility if the required reasonable experimental resources can be focused on this project.

Even on a much more modest mass level, in the range between 500 and 10.000 amu, there is a plethora of molecules that only wait for being subjected to quantum interferometry. We have already seen that matter interferometry allows us to determine static and optical polarizabilities with good precision. Already these scalar values provide relevant information that may help identifying or separating [99] molecular conformers of different amino acid or nucleotide sequences, i.e. of polypeptides, oligonucleotides or short DNA strands.

Structural and conformation changes in free flight may become measurable. An example for that would be the trans-cis isomerization in azobenzene derivatives or retinal. Their different conformers are connected with different polarizabilities and dipole moments and thus affect the highly sensitive molecule grating interaction. Interferometry may thus become an interesting complementary tool to mass spectrometry and optical spectroscopy.

The Vienna experiments have proven that quantum interference is feasible in spite of the substantial internal excitations present in complex molecules. On the other hand, the investigations also show that further slowing and cooling will be required in future experiments to pave the path to interferometry with supermassive clusters and highly complex molecules. Only internal state cooling will allow us to play with new ideas on internal-external state entanglement. Highly efficient cryogenic techniques will probably have to be complemented by new quantum optical manipulation ideas.

In variance of Feynman’s early statement on nanotechnology [103] we therefore think: *There is plenty of room at the top.*

\* \* \*

The scientific program on macromolecular interference was started in collaboration between one of the authors (MA) and Anton Zeilinger. Over the years, work on interferometry with fullerenes and large molecules has benefited enormously from important contributions by many bright students, postdocs and collaborators, as documented in the references. Our research has been supported by the Austrian FWF within the programs SFB F1505, START Y177, Wittgenstein Z149 and COQUS, by the European Commis-

sion within the IHP network QUACS and the ESF programme EuroQuasar MIME, and by the DFG Emmy Noether programme.

## REFERENCES

- [1] DE BROGLIE L., *Nature* , **112** (1923) 540.
- [2] PLANCK M., *Verhandl. Dtsch. phys. Ges.* , **2** (1900) 237 .
- [3] EINSTEIN A., *Ann. Physik* , **17** (1905) 132.
- [4] SCHRÖDINGER E., *Annalen der Physik* , **79** (1926) 361.
- [5] DAVISSON C. and GERMER L., *Nature* , **119** (1927) 558 .
- [6] THOMSON G. P., *Nature* , **120** (1927) 802.
- [7] MISSIROLI G. F., POZZI G. and VALDRE U., *J. Phys. E* , **14** (1982) 649.
- [8] HOVE M. A. V. and TONG S. Y., *Surface crystallography by LEED* (Springer-Verlag New York) 1979.
- [9] GABOR D., *Nature* , **161** (1948) 777 .
- [10] TONOMURA A., *Rev. Mod. Phys.* , **59** (1987) 639.
- [11] BINNIG G., ROHER H., GERBER C. and WEIBEL E., *Phys. Rev. Lett.* , **50** (1983) 120.
- [12] CROMMIE M. F., LUTZ C. and EIGLER D., *Science* , **262** (1993) 218.
- [13] JI Y., CHUNG Y., SPRINZAK D., HEIBLUM M., MAHALU D. and SHTRIKMAN H., *Nature* , **422** (2003) 415 .
- [14] SONNENTAG P. and HASSELBACH F., *Phys. Rev. Lett.* , **98** (2007) 200402.
- [15] GRONNIGER G., BARWICK B., BATELAAN H., SAVAS T., PRITCHARD D. and CRONIN A., *Appl. Phys. Lett.* , **87** (2005) 124104.
- [16] ESTERMANN I. and STERN O., *Z. Phys.* , **61** (1930) 95.
- [17] CHADWICK J., *Nature* , **129** (1932) 798.
- [18] HALBAN JNR H. and PREISWERK P., *Comptes Rendus Acad. Sci. Paris* , **203** (1936) 73.
- [19] SHULL C. G., *Rev. Mod. Phys.* , **67** (1995) 753.
- [20] BROCKHOUSE B. N., *Rev. Mod. Phys.* , **67** (1995) 735.
- [21] SEARS V. F., *Neutron optics : an introduction to the theory of neutron optical phenomena and their applications*, Oxford series on neutron scattering in condensed matter, Vol. 3 (Oxford University Press) 1989.
- [22] RAUCH H. and WERNER A., *Neutron Interferometry: Lessons in Experimental Quantum Mechanics* (Oxford Univ. Press) 2000.
- [23] GOULD P. L., RUFF G. A. and PRITCHARD D. E., *Phys. Rev. Lett.* , **56** (1986) 827 .
- [24] MARTIN P. J., OLDAKER B. G., MIKLICH A. H. and PRITCHARD D. E., *Phys. Rev. Lett.* , **60** (1988) 515.
- [25] KEITH D. W., SCHATTEBURG M. L., SMITH H. I. and PRITCHARD D. E., *Phys. Rev. Lett.* , **61** (1988) 1580.
- [26] CARNAL O. and MLYNEK J., *Phys. Rev. Lett.* , **66** (1991) 2689.
- [27] KEITH D. W., EKSTROM C. R., TURCHETTE Q. A. and PRITCHARD D. E., *Phys. Rev. Lett.* , **66** (1991) 2693.
- [28] KASEVICH M., WEISS D. S., RIIS E., MOLER K., KASAPI S. and CHU S., *Phys. Rev. Lett.* , **66** (1991) 2297.
- [29] EKSTROM C., SCHMIEDMAYER J., CHAPMAN M., HAMMOND T. and PRITCHARD D., *Phys. Rev. A* , **51** (1995) 3883.
- [30] MIFFRE A., JACQUEY M., BÜCHNER M., TRÉNEC G. and VIGUÉ J., *Phys. Rev. A* , **73** (2006) 011603(R).

- [31] KASEVICH M. and CHU S., *Phys. Rev. Lett.* , **69** (1992) 1741.
- [32] PETERS A., KENG-YEOW-CHUNG and CHU S., *Nature* , **400** (1999) 849.
- [33] RIEHLE F., KISTERS T., WITTE A., HELMCKE J. and BORDE C. J., *Phys. Rev. Lett.* , **67** (1991) 177.
- [34] GUSTAVSON T. L., BOUYER P. and KASEVICH M. A., *Phys. Rev. Lett.* , **78** (1997) 2046.
- [35] WEISS D., YOUNG B. and CHU S., *Phys. Rev. Lett.* , **70** (1993) 2706.
- [36] SCHMIEDMAYER J., CHAPMAN M., EKSTROM C., HAMMOND T., WEHINGER S. and PRITCHARD D., *Phys. Rev. Lett.* , **74** (1995) 1043.
- [37] BORDÉ C., COURTIER N., BURCK F. D., GONCHAROV A. and GORLICKI M., *Phys. Lett. A* , **188** (1994) 187.
- [38] SCHÖLLKOPF W. and TOENNIES J. P., *Science* , **266** (1994) 1345.
- [39] CHAPMAN M. S., EKSTROM C. R., HAMMOND T. D., RUBENSTEIN R. A., SCHMIEDMAYER J., WEHINGER S., and PRITCHARD D. E., *Phys. Rev. Lett.* , **74** (1995) 4783 .
- [40] INGUSCIO M., STRINGARI S. and WIEMAN C. (Eds.), *Bose-Einstein Condensation in Atomic Gases* (Italian Physical Society) 1999.
- [41] INGUSCIO M., KETTERLE W. and SALOMON C. (Eds.), *Ultra-Cold Fermi Gases, Proceedings of the International School of Physics Enrico Fermi Course CLXIV* (IOS Press Amsterdam) 2008.
- [42] DALFOVO F., GIORGINI S., PITAEVSKII P. and STRINGARI S., *Rev. Mod. Phys.* , **71** (1999) 463 .
- [43] LEGGETT A. J., *Rev. Mod. Phys.* , **73** (2001) 307 .
- [44] PETHICK C. J. and SMITH H., *Bose-Einstein Condensation in Dilute Gases* (Cambridge University Press, Cambridge) 2002.
- [45] PITAEVSKI L. and STRINGARI S., *Bose-Einstein Condensation* (Oxford University Press) 2003.
- [46] BLOCH I., DALIBARD J. and ZWGER W., *Rev. Mod. Phys.* , **80** (2008) 885.
- [47] ADAMS C. S., SIEGEL M. and MLYNEK, J., *Phys. Rep.*, **240** (1994) 143.
- [48] ZEH H.-D., *Found. Phys.* , **3** (1973) 109.
- [49] ZUREK W. H., *Phys. Today* , **44** (1991) 36.
- [50] BASSI A. and GHIRARDI G., *Phys. Rep.* , **379** (2003) 257.
- [51] SCHLOSSHAUER M., *Rev. Mod. Phys.* , **76** (2004) 1267.
- [52] PENROSE R., *Gen. Rel. Grav.* , **28** (1996) 581.
- [53] LEGGETT A. J., *J. Phys.: Condens. Matter* , **14** (2002) R415.
- [54] WANG C., BINGHAM R. and MENDONCA J. T., *Class. Quant. Grav.* , **23** (2006) L59.
- [55] CARLIP S., *Quantum Grav.*, **25** (2008) 154010.
- [56] WANG C. H.-T., BONIFACIO P. M., BINGHAM R. and MENDONCA J. T., *eprint* , (2008) arXiv:0806.3042.
- [57] ARNDT M., HACKERMÜLLER L. and ZEILINGER A., *Molecule interferometry as a potential tool for nanostructuring applications*, in *Proceedings of the 4th EC/NSF Workshop on Nanotechnology, Tools and Instruments for Research and Manufacturing, Grenoble, France, June 12.-13.th (2002)* 2002.
- [58] MESCHEDE D. and METCALF H., *J. Phys. D: Appl. Phys.* , **36** (2003) R17 .
- [59] BETHLEM H. L., BERDEN G. and MEIJER G., *Phys. Rev. Lett.* , **83** (1999) 1558.
- [60] BOCHINSKI J. R., HUDSON E. R., LEWANDOWSKI H. J., MEIJER G. and YE J., *Phys. Rev. Lett.* , **91** (2003) 243001.
- [61] HEINER C. E., CARTY D., MEIJER G. and BETHLEM H. L., *Nature Physics* , **3** (2007) 115 .
- [62] GANGL M. and RITSCH H., *Phys. Rev. A* , **61** (2000) 011402/1.

- [63] LEV B. L., VUKICS A., HUDSON E. R., SAWYER B. C., DOMOKOS P., RITSCH H. and YE J., *arXiv:0705.3639v1 [quant-ph]*, (2007) .
- [64] NAIRZ O., ARNDT M. and ZEILINGER A., *Am. J. Phys.*, **71** (2003) 319.
- [65] KOLODNEY E., TSIPINYUK B. and BUDREVICH, A., *J. Chem. Phys.*, **102** (1995) 9263.
- [66] ARNDT M., NAIRZ O., VOSS-ANDREAE J., KELLER C., DER ZOUW G. V. and ZEILINGER A., *Nature*, **401** (1999) 680.
- [67] NAIRZ O., BREZGER B., ARNDT M. and ZEILINGER A., *Phys. Rev. Lett.*, **87** (2001) 160401.
- [68] PFAU T., SPÄLTER S., KURTSIEFER C., EKSTROM C. and MLYNEK J., *Phys. Rev. Lett.*, **73** (1994) 1223.
- [69] TALBOT H. F., *Philos. Mag.*, **9** (1836) 401.
- [70] LAU E., *Ann. Phys. (Paris)*, **6** (1948) 417.
- [71] CLAUSER J. F. and LI S., *Phys. Rev. A*, **49** (1994) R2213.
- [72] CLAUSER J., *De Broglie-wave interference of small rocks and live viruses*, in *Experimental Metaphysics*, edited by COHEN R., HORNE M. and STACHEL J. (Kluwer Academic) 1997, pp. 1–11.
- [73] BREZGER B., HACKERMÜLLER L., UTTENTHALER S., PETSCHINKA J., ARNDT M. and ZEILINGER A., *Phys. Rev. Lett.*, **88** (2002) 100404.
- [74] HORNBERGER K., SIPE J. E. and ARNDT M., *Phys. Rev. A*, **70** (2004) 53608.
- [75] NIMMRICHTER S. and HORNBERGER K., *Phys. Rev. A*, **78** (2008) 023612.
- [76] HACKERMÜLLER L., UTTENTHALER S., HORNBERGER K., REIGER E., BREZGER B., ZEILINGER A. and ARNDT M., *Phys. Rev. Lett.*, **91** (2003) 90408.
- [77] GERLICH S., GRING M., ULBRICHT H., HORNBERGER K., TÜXEN J., MAYOR M. and ARNDT M., *Angew. Chem. Int. Ed.*, **47** (2008) 6195.
- [78] GERLICH S., HACKERMÜLLER L., HORNBERGER K., STIBOR A., ULBRICHT H., GRING M., GOLDFARB F., SAVAS T., MÜRI M., MAYOR M. and ARNDT M., *Nature Physics*, **3** (2007) 711 .
- [79] KAPITZA P. L. and DIRAC P. A. M., *Proc. Camb. Philos. Soc.*, **29** (1933) 297 .
- [80] N. DOLTSINIS, *Kings College London*, (priv. comm., 2008) .
- [81] JOOS E., ZEH H. D., KIEFER C., GIULINI D., KUPSCH J. and STAMATESCU I.-O., *Decoherence and the Appearance of a Classical World in Quantum Theory*, 2nd Edition (Springer, Berlin) 2003.
- [82] SCHLOSSHAUER M., *Decoherence and the Quantum-to-Classical Transition*, The Frontiers Collection (Springer Verlag) 2007.
- [83] HORNBERGER K., *Introduction to decoherence theory*, in *Entanglement and Decoherence. Foundations and Modern Trends*, edited by BUCHLEITER A., VIVIESCAS C. and TIERSCH, M., *Lecture Notes in Physics*, **768** (Springer, Berlin 2009) 221-276.
- [84] HORNBERGER K., UTTENTHALER S., BREZGER B., HACKERMÜLLER L., ARNDT M. and ZEILINGER A., *Phys. Rev. Lett.*, **90** (2003) 160401.
- [85] HACKERMÜLLER L., HORNBERGER K., BREZGER B., ZEILINGER A. and ARNDT M., *Nature*, **427** (2004) 711.
- [86] ARNDT M., HORNBERGER K. and ZEILINGER A., *Physics World*, **18 (3)** (2005) 35.
- [87] HORNBERGER K. and SIPE J. E., *Phys. Rev. A*, **68** (2003) 12105.
- [88] HACKERMÜLLER L., HORNBERGER K., BREZGER B., ZEILINGER A. and ARNDT M., *Appl. Phys. B*, **77** (2003) 781.
- [89] VACCHINI B., *J. Mod. Opt.*, **51** (2004) 1025.
- [90] CHAMPENOIS C., JACQUEY M., LÉPOUTRE S., BÜCHNER M., TRÉNEC G. and VIGUÉ J., *Phys. Rev. A*, **77** (2008) 013621.
- [91] HORNBERGER K. and VACCHINI B., *Phys. Rev. A*, **77** (2008) 022112.

- [92] JACQUEY M., BÜCHNER M., TRÉNEC G. and VIGUÉ J., *Phys. Rev. Lett.* , **98** (2007) 240405.
- [93] HORNBERGER K., HACKERMÜLLER L. and ARNDT M., *Phys. Rev. A* , **71** (2005) 023601.
- [94] STIBOR A., HORNBERGER K., HACKERMÜLLER L., ZEILINGER A. and ARNDT M., *Laser Physics* , **15** (2005) 10.
- [95] BERNINGER M., STÉFANOV A., DEACHAPUNYA S. and ARNDT M., *Phys. Rev. A* , **76** (2007) 013607.
- [96] HACKERMÜLLER L., HORNBERGER K., GERLICH S., GRING M., ULBRICHT H. and ARNDT M., *Applied Physics B* , **89** (2007) 469
- [97] CHAPMAN M. S., EKSTROM C. R., HAMMOND T. D., RUBENSTEIN R. A., SCHMIEDMAYER J., WEHINGER S. and PRITCHARD D. E., *Phys. Rev. Lett.* , **74** (1995) 4783.
- [98] STEFANOV A., BERNINGER M. and ARNDT M., *Meas. Sci. Technol.* , **19** (2008) 055801.
- [99] ULBRICHT H., BERNINGER M., DEACHAPUNYA S., STEFANOV A. and ARNDT M., *Nanotechnology* , **19** (2008) 045502.
- [100] STIBOR A., STEFANOV A., GOLDFARB F., REIGER E. and ARNDT M., *New Journal of Physics* , **7** (2005) 1.
- [101] BECKER C. H. and WU K. J., *J. Am. Soc. Mass Spectrom.* , **6** (1995) 883 .
- [102] MARKSTEINER M., HASLINGER P., ULBRICHT H., SCLAFANI M., OBERHOFFER H., DELLAGO C. and ARNDT M., *J. Am. Soc. Mass. Spectrom.* , **19** (2008) 1021 .
- [103] R. FEYNMAN, *APS meeting*, (Caltech, Pasadena) 1959;  
<http://www.zyvex.com/nanotech/feynman.html>.